PHYSICAL REVIEW B VOLUME 45, NUMBER 23 15 JUNE 1992-I

Structural and elastic properties of transition-metal superlattices

R. S. Jones and J. A. Slotwinski
Department of Physics, Loyola College, Baltimore, Maryland 20210

J. W. Mintmire
Chemistry Division, U.S. Naval Research Laboratory, Washington, D.C. 20375
(Received 31 January 1992)

We have calculated the equilibrium geometries and elastic properties of transition-metal superlattices (Cu-Ni, Cu-Pd, and Cu-Au) over a range of composition modulation wavelengths for both slab-layered systems (with alternating equal-width slabs of the constituents) and for systems with a sinusoidally modulated composition. The energies and equilibrium geometries were obtained with the embedded-atom method and the elastic constants were determined both by considering appropriate sums over the dynamical matrix and by calculating the energy of specific deformations of the unit cell. No enhancements of the elastic constants or moduli were found for any of the systems considered, in agreement with recent experimental results.

INTRODUCTION

The presence of structural defects in a metal is important in determining nonlinear mechanical properties such as yield strength and flow, but the linear properties such as the elastic moduli are generally found to be insensitive to the microscopic structural details. Earlier experimental results,[1-4] however, suggested that for a layered superlattice of different metals, certain elastic moduli may be strongly dependent on the details of the superlattice structure. This is the so-called "supermodulus" effect, in which some elastic moduli may be enhanced for particular superlattice wavelengths. A great deal of attention has been focused on investigating the detailed structural properties of the interfaces is these systems.[5,6] Recent experimental results[7-10] have indicated that the effect on the elastic properties in much smaller than originally described, but interest in the microscopic nature of the interfaces, and their contribution to elastic properties, remains.

For the alloys of noble metals and near-noble transition metals considered here, it is evident that the layers are coherent at sufficiently small modulation wavelength. As the modulation wavelength increases, we expect the systems to undergo a transition to an incoherent state. In the coherent state, elastic properties will be affected by the strained nature of the two metals,[11] and the local disorder at the interface.[12,13] In the incoherent state, elastic properties will be affected by the increased disorder at the interface.[14,15] Detailed calculations of the incoherent state, however, are extremely difficult, because the small lattice mismatch between metal species requires a very large number of atoms for the simulation to allow the use of periodic boundary conditions,[16] or to minimize surface effects.[17] Calculations to date have utilized mostly model interactions with artificially large lattice mismatches to reduce the size of the system.[15] Alternatively, grain boundaries in pure metals have been considered as representative of the effects that boundaries may have on elastic properties.[18,19]

Banarjea and Smith[20] studied the Cu-Ni system within a continuum model using experimentally derived elastic constants, and Dodson[21] looked briefly at [100]-layered systems. Herein, we present definitive results for transition-metal–noble-metal alloy systems that are constrained to form coherent interfaces. Preliminary results have been presented elsewhere for our work on a particular Cu-Ni multilayered system.[22] We are currently investigating structural and elastic results for incoherent lattices. These results will be reported at a later time.

DESCRIPTION OF SYSTEMS AND COMPUTATIONAL METHODS

The superlattice was modeled using close-packed layers in the fcc [111]-layered structure with periodic boundary conditions applied in all directions. Within each cell, 6–24 layers were used, each containing 30 atoms. We considered two types of composition modulation: slab-layered composition with blocks of several monoelemental layers, and sinusoidal modulation with the composition of each layer varying as a sine function. Modulation wavelengths (in terms of the number of layers, Λ, in a repeat unit) of between 4 and 24 atomic planes were considered for slab-layered systems with sharply varying composition, and for sinusoidally modulated systems with smoothly varying composition. Slab systems consisted of alternating blocks of $\Lambda/2$ layers of each constituent. For the sinusoidal configurations, the number of atom species A in the ith plane was determined from the nearest integer to the expression

$$N_i(A)=\{[1+\sin(i/\Lambda)]N_{\rm tot}/2\},$$

where $N_{\rm tot}$ is the total number of atoms in each layer. The atoms in each layer were then randomly assigned to lattice sites. A minimum of ten systems was generated

with the same composition wavelength, and all properties were determined as averages over these systems. Note that both slab and sinusoidal systems contain equal numbers of atoms of the two constituents in all cases considered. Systematic studies were performed on three materials: Cu-Ni, Cu-Pd, and Cu-Au.

The energies and equilibrium geometries were obtained with the embedded-atom method (EAM).[23] The embedded-atom potentials used were those optimized for the six metals: Cu, Ni, Au, Ag, Pd, and Pt.[24] For the Cu-Ni system, we also considered the potentials optimized specifically for this system.[25] In this study, very little difference was found between these two forms of the potential, although this is not always the case.[26] Minimum-energy structures were determined by relaxing both the periodic boundary lengths and the positions of all atoms within the cell, using a direct minimization technique.

Elastic constants were calculated directly from the appropriate second derivatives of the energy with respect to strain. These derivatives were performed using the expressions derived by Lutsko[27] at zero atomic stress, so that the internal relaxation of atoms within the crystal is allowed. An independent check of these results was made by determining the elastic constants via a finite strain method, in which the energy is calculated as a function of specific deformations of the periodic cell, and elastic constants are determined from the curvature of the energy versus strain curves. The biaxial (Y_B), flexural (Y_F), and Young's (Y_Y) elastic moduli are obtained from the elastic constants according to the following formulas:[28]

$$Y_B = c_{11} + c_{12} - 2c_{13}^2/c_{33} ,$$

$$Y_F = c_{11} - c_{13}^2/c_{33} ,$$

$$Y_Y = \frac{(c_{11}-c_{12})[c_{33}(c_{11}+c_{12})-2c_{13}^2]}{(c_{11}-c_{33}-c_{13}^2)} .$$

Note that Y_Y is the in-plane Young's modulus. These formulas are appropriate for a system with rhombohedral symmetry, with the superlattice layers lying in the xy plane.

STRUCTURAL RESULTS

We will present detailed structural results only for the Cu-Ni system because the results for all three materials were very similar.

The equilibrium arrangement of the slab system is shown in Fig. 1 for a modulation wavelength of 12 atomic layers. Note that the shift in plane separation from an equally spaced lattice has been exaggerated in this picture by a factor of 10, to make the difference in separation more apparent. The actual spacing between planes for this system is given in Table I and shown in Fig. 2. The periodic boundary conditions restrict the system to be coherent so that the in-plane, nearest-neighbor distance is the same for both Cu and Ni planes. This distance is 2.5209 Å for large Λ, representing a 1.3% expansion for Ni and a 1.2% compression for Cu as compared to bulk values. As expected from the Poisson ratios of the two

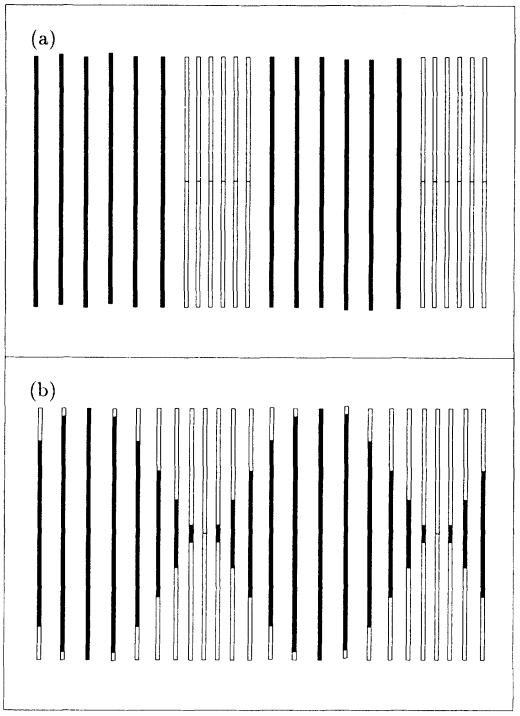

FIG. 1. Cu-Ni in (a) a slab-layered superlattice and (b) a sinusoidally modulated superlattice for $\Lambda=12$ atomic layers. The fraction of the plane occupied by Cu atoms is indicated by black bars. Note that the shift in interplanar separation from an equally spaced lattice has been exaggerated by a factor of 10.

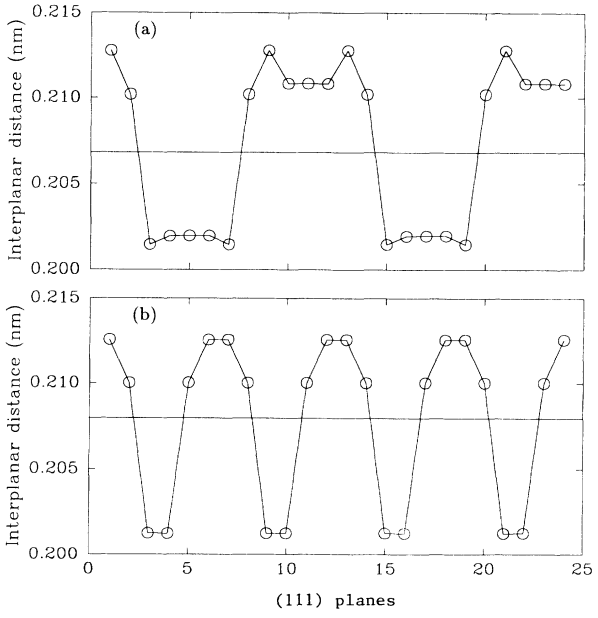

FIG. 2. Distance between (111) planes for a Cu-Ni slab system with (a) $\Lambda=12$ and (b) $\Lambda=6$ atomic layers. Data points have been connected with lines to aid the eye. The horizontal line is the averaged plane separation.

TABLE I. Interplanar separation for a Cu-Ni slab-layered superlattice.

$\Lambda=12$		$\Lambda=6$	
Interface type	Interplanar separation (Å)	Interface type	Interplanar separation (Å)
Ni-Ni	2.0146	Ni-Ni	2.0127
Ni-Ni	2.0195	Ni-Ni	2.0128
Ni-Ni	2.0197	Ni-Cu	2.1003
Ni-Ni	2.0197	Cu-Cu	2.1257
Ni-Ni	2.0197	Cu-Cu	2.1257
Ni-Cu	2.0197	Cu-Ni	2.1003
Cu-Cu	2.1278	Ni-Ni	2.0127
Cu-Cu	2.1082	Ni-Ni	2.0128
Cu-Cu	2.1083	Ni-Cu	2.1003
Cu-Cu	2.1082	Cu-Cu	2.1256
Cu-Cu	2.1278	Cu-Cu	2.1256
Cu-Ni	2.1021	Cu-Ni	2.1003
Average	2.0683	Average	2.0796
Average in-plane nearest-neighbor separation	2.5209		2.5240

metals, these in-plane strains lead to interplanar strains of opposite sign: a decrease in the interplanar separation within the Ni slabs of 0.6%, and an expansion within the Cu slabs of 1.2%.

In Fig. 2, we see that the interface width is essentially limited to the two layers on either side of the boundary. There is considerably more structure in this interface than was found by Phillpot and Wolf[13] in a consideration of (100) coherent interfaces using Lennard-Jones potentials. It is not clear whether the difference is the result of the plane orientation, or the choice of interatomic potentials. Recent calculations, however, of thin-film elastic properties with both Lennard-Jones and EAM potentials, have been found to give very different results.[29] The increased separation between the two Cu-Cu planes at the boundary, and the fact that the separation between the Cu and Ni planes at the interface is larger than the average spacing (shown as the horizontal line in Fig. 2), has the net result that the interface is 0.052 Å thicker than the bulk.

The form of the interface region was found to be nearly independent of the modulation wavelength, even down to $\Lambda=6$ layers as shown in Fig. 2, where the bulk region has essentially disappeared, but the interface maintains a nearly identical structure. The effective thickness of the interface is the primary factor responsible for the increase in the average plane separation of the superlattice as Λ decreases. An additional factor, however, is the slight increase (0.1%) in the in-plane nearest-neighbor separation as Λ goes from 24 to 6, which can be attributed to an "interface compressive stress" that generates the expansion when the density of interfaces increases. This increase of the in-plane separation is accompanied by a decrease in the interplanar separation in the bulk regions, as dictated by the Poisson ratios of the bulk materials.

The equilibrium arrangement of the sinusoidal system is shown in Fig. 1(b) for a modulation wavelength of 12 atomic layers. The actual spacing between planes for a single calculation (i.e., one set of random occupations of the layer sites) of this system is given in Table II and shown in Fig. 3. The layer separation follows the composition profile very closely, coming very near the bulk values of the separation from the slab configuration for the planes that are composed of a single constituent. The sinusoidal composition modulation has widened the interfaces, so that we cannot precisely define interface and bulk regions for these systems. It is interesting to note that the dependence on Λ of the average dimensions of the system (as shown in Table II) is very similar to that of

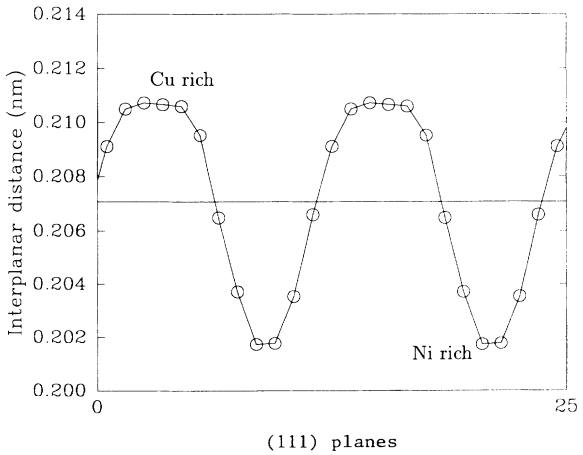

FIG. 3. Distance between (111) planes for a Cu-Ni sinusoidally modulated superlattice for $\Lambda=12$ atomic layers. Data points have been connected with lines to aid the eye. The horizontal line is the average plane separation.

TABLE II. Interplanar separation for a Cu-Ni sinusoidally modulated superlattice.

Λ=12			Λ=6		
Percentage Cu in adjacent planes		Interplanar separation	Percentage Cu in adjacent planes		Interplanar separation
50%	73%	2.0911	50%	93%	2.1024
73%	93%	2.1049	93%	93%	2.1196
93%	100%	2.1072	93%	50%	2.1018
100%	93%	2.1065	50%	7%	2.0540
93%	73%	2.1059	7%	7%	2.0188
73%	50%	2.0952	7%	50%	2.0531
50%	27%	2.0649	50%	93%	2.1017
27%	7%	2.0371	93%	93%	2.1181
7%	0%	2.0173	93%	50%	2.1011
0%	7%	2.0177	50%	7%	2.0518
7%	27%	2.0354	7%	7%	2.0191
27%	50%	2.0660	7%	50%	2.0533
Average		2.0708	Average		2.0746
Average in-plane nearest-neighbor separation		2.5327			2.5348

the slab systems. Specifically, as the number of interfaces increases, the average layer spacing increases, and the average in-plane nearest-neighbor separation increases. This effect is smaller for the sinusoidal system than for the slab system, which presumably results from the more diffuse nature of the interfaces.

For these sinusoidal systems, we can also compare the in-plane nearest-neighbor separations between different atomic species, a comparison not possible for the slab-layered systems. We find that in layers containing 50% of each constituent, the Cu atoms tend to move away from each other, and Ni atoms tend to move closer. This results in an increase of approximately 0.5% in the average in-plane Cu-Cu nearest-neighbor distance, and a decrease of approximately 1.5% for the Ni-Ni distance. Because the difference in bulk bond lengths is only 2.5%, this is a significant shift. Thus, although the system has long-range coherence that constrains the average nearest-neighbor distance to be identical for all layers, the statistical distribution of atomic sites at the interfaces results in a local disorder that allows adjacent homonuclear pairs of atoms to tend toward their bulk separations. This local disorder is present even for small-wavelength systems where a coherent lattice is the preferred configuration, and so does not seem to be an artifact of the coherency constraint.

Structural results for Cu-Pd and Cu-Au were very similar, with the exception that the dimensional trends were not as well defined in the Cu-Au systems. The lattice spacings have a much greater mismatch in these two systems than in the Cu-Ni system. This effect appears to result in the interfacial compression detailed above: the average in-plane separation r_{NN} decreases with decreasing Λ, while the average interplanar separation r_z increases.

ELASTIC PROPERTIES

The calculated elastic moduli for Cu-Ni, Cu-Pd, and Cu-Au in the sinusoidal geometries are shown in Fig. 4 and tabulated in Table III. As the modulation wavelength goes from 24 atomic layers to 4 layers, all of these moduli monotonically decrease by a few percent. The elastic constants showed a similar weak dependence on Λ. The internal relaxation contribution was found to be very small (less than 1%) for these systems. Note that

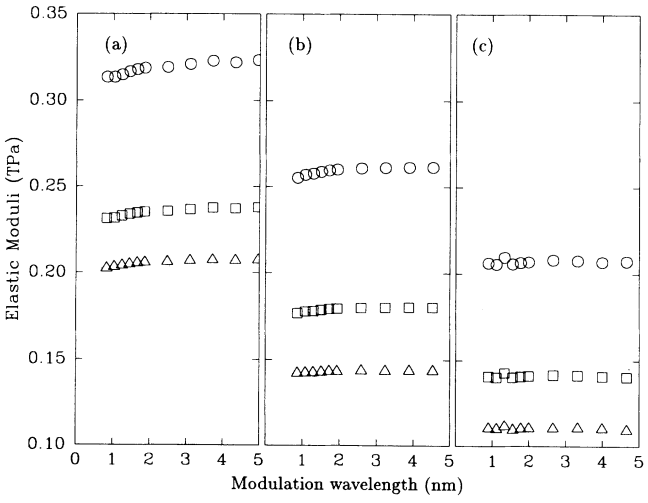

FIG. 4. Elastic moduli for (a) Cu-Ni, (b) Cu-Pd, and (c) Cu-Au for sinusoidal configurations. Data points are given by circles, squares, and triangles for the biaxial (Y_B), flexural (Y_F), and in-plane Young's (Y_Y) elastic moduli, respectively.

this contribution always serves to decrease the moduli.

For the slab geometries, the results are similar, although the overall decreases in the moduli as Λ goes from 24 to 4 atomic layers are as large as 8% in some cases. Representative results for Cu-Ni are shown in Table IV. The decreases in the moduli as Λ goes from 24 to 6 atomic layers are 3%, 5%, and 8%, respectively, for the biaxial, flexural, and Young's moduli. The contribution of the relaxation term to the elastic moduli was larger for the smaller-wavelength slab systems as is indicated for $\Lambda=6$, where the relaxation contribution accounts for $\frac{1}{2}$ to $\frac{3}{4}$ of the decrease in the moduli. The interfaces clearly make the major contribution to the relaxation term.

The simplest approach to predicting the elastic moduli of these systems from the known bulk properties of the pure metals is a simple average. An average based on a method due to Grimsditch[30] has been popular as a predictor of effective moduli, but this method will not apply to these systems, because this scheme was determined by assuming that the interfaces play no role in determining the moduli. This is certainly not the case for the coherent superlattices. The elastic moduli of the pure metals calculated with the EAM are shown in Table IV, along with the averages for the three systems considered. Note that in all cases the actual elastic moduli of all systems are smaller than the average moduli of the pure metals, even in the large-wavelength limit. The reason lies in the strained nature of the materials even for large Λ, due to the periodic boundary conditions.

An improved predictor of the elastic moduli is to average the moduli of pure metals in strained states corresponding to the superlattice structure. This can only be done for slab systems where we know the bulk lattice constants of each component. Results for the Cu-Ni slab system are included in Table IV. First note that for Cu, the intraplane expansion combined with the interplane compression serves to increase the elastic moduli over that of the bulk material. The opposite strains in the Ni system decrease the moduli. Because the increase in Cu

TABLE III. Average calculated elastic moduli of composition-modulated systems with sinusoidal composition profiles.

System	Λ	r_{NN} (Å)	r_z (Å)	Biaxial (TPa)	Flexural (TPa)	Young's (TPa)
Cu-Ni	24	2.5319	2.0704	0.3234	0.2381	0.2075
	21	2.5317	2.0705	0.3220	0.2374	0.2072
	18	2.5317	2.0704	0.3229	0.2378	0.2074
	15	2.5321	2.0708	0.3210	0.2368	0.2069
	12	2.5324	2.0712	0.3192	0.2358	0.2063
	9	2.5327	2.0720	0.3188	0.2354	0.2059
	8	2.5328	2.0727	0.3180	0.2349	0.2056
	7	2.5331	2.0735	0.3168	0.2341	0.2049
	6	2.5341	2.0750	0.3149	0.2330	0.2041
	5	2.5350	2.0772	0.3135	0.2319	0.2032
	4	2.5352	2.0816	0.3135	0.2315	0.2024
Cu-Pd	24	2.6748	2.1680	0.2616	0.1805	0.1439
	21	2.6748	2.1675	0.2615	0.1804	0.1438
	18	2.6750	2.1672	0.2614	0.1803	0.1438
	15	2.6751	2.1671	0.2612	0.1802	0.1437
	12	2.6756	2.1663	0.2609	0.1800	0.1438
	9	2.6767	2.1644	0.2601	0.1795	0.1433
	8	2.6774	2.1633	0.2596	0.1793	0.1433
	7	2.6784	2.1617	0.2588	0.1788	0.1430
	6	2.6789	2.1609	0.2577	0.1781	0.1426
	5	2.6812	2.1588	0.2570	0.1778	0.1425
	4	2.6831	2.1546	0.2552	0.1769	0.1423
Cu-Au	24	2.7599	2.2251	0.2080	0.1416	0.1104
	21	2.7610	2.2282	0.2073	0.1407	0.1094
	18	2.7594	2.2202	0.2069	0.1410	0.1103
	15	2.7579	2.2206	0.2077	0.1416	0.1107
	12	2.7579	2.2260	0.2081	0.1417	0.1105
	9	2.7593	2.2182	0.2069	0.1412	0.1106
	8	2.7599	2.2173	0.2065	0.1408	0.1103
	7	2.7608	2.2184	0.2057	0.1403	0.1097
	6	2.7571	2.2211	0.2096	0.1429	0.1117
	5	2.7620	2.2121	0.2055	0.1404	0.1102
	4	2.7621	2.2117	0.2062	0.1409	0.1105

TABLE IV. Results for Cu-Ni in a slab-layered superlattice. Elastic moduli of pure metals in equilibrium lattices and strained lattices are also included as a comparison with the superlattice values. An asterisk denotes no internal relaxation allowed in the calculation of moduli.

Material	Λ	r_{NN} (Å)	r_z (Å)	Biaxial (TPa)	Flexural (TPa)	Young's (TPa)
Cu (bulk)		2.553	2.084	0.2700	0.1951	0.1664
Ni (bulk)		2.490	2.033	0.3996	0.3003	0.2675
Pd (bulk)		2.751	2.246	0.2707	0.1844	0.1440
Au (bulk)		2.885	2.356	0.1981	0.1330	0.1012
Cu-Ni (average)				0.3348	0.2477	0.2170
Cu-Pd (average)				0.2704	0.1896	0.1548
Cu-Au (average)				0.2341	0.1639	0.1334
Cu-Ni (slab)	24	2.521	2.068	0.3278	0.2416	0.2108
Cu (strained)		2.521	2.108	0.3183	0.2300	0.1962
Ni (strained)		2.521	2.020	0.3362	0.2529	0.2255
Cu-Ni (average)				0.3273	0.2415	0.2108
Cu-Ni* (slab)	6	2.524	2.080	0.3224	0.2374	0.2069
Cu-Ni (slab)	6	2.524	2.080	0.3177	0.2288	0.1942
Cu (strained)		2.524	2.108	0.3133	0.2263	0.1928
Ni (strained)		2.524	2.020	0.3301	0.2483	0.2213
Cu-Ni (average)				0.3217	0.2373	0.2070

is less than the decrease in Ni for each of the three moduli, the average of the strained values is less than the average of the bulk values, and gives a very close approximation to all three of the elastic moduli at $\Lambda=24$. At $\Lambda=6$, the small changes in lattice constants account for the changes in all the elastic moduli if we do not allow for internal relaxation. Because internal relaxation terms always serve to decrease the moduli, the actual elastic moduli are slightly less than the values predicted by dimensional changes alone.

SUMMARY

We have calculated the equilibrium geometries and elastic properties within the embedded-atom method for the Cu-Ni, Cu-Pd, and Cu-Au transition-metal superlattices over a range of composition modulation wavelengths for both slab-layered systems and for sinusoidally modulated systems. No enhancements of the elastic constants or moduli were found for any of the systems considered, in agreement with recent experimental results. The effects of the relaxation of nuclear positions under strain on the elastic constants were incorporated into the calculations, and we found these effects were minor and led to no qualitative changes in our results.

Although the calculations herein assumed a coherent lattice, a trend toward an incoherent interface was noted in the sinusoidally modulated calculations, in the relative separations between atoms of the same species. Our results indicate an initial phase of structural disorder at the coherent interface, and demonstrate a clear need to consider larger systems to observe this tendency toward structural disorder, with the possible development of incoherent interfaces. This will require systems without periodic boundary conditions in directions transverse to the superlattice periodicity, and at a scale large enough to diminish surface effects. Preliminary work in this area has begun.

ACKNOWLEDGMENTS

This work was supported in part by the U.S. Office of Naval Research. Computational support for this project was provided in part by a grant of computer resources from the Naval Research Laboratory.

[1]T. Tsakalakos, J. Vac. Sci. Technol. B **4**, 1447 (1986).
[2]A. Jankowski and T. Tsakalakos, J. Appl. Phys. **57**, 1835 (1985).
[3]T. Tsakalakos and J. E. Hilliard, J. Appl. Phys. **54**, 734 (1983).
[4]D. Baral, J. B. Ketterson, and J. E. Hilliard, J. Appl. Phys. **54**, 1076 (1985).
[5]C. Kim, S. B. Qadri, M. Twigg, and A. S. Edelstein, J. Vac. Sci. Technol. A **8**, 3466 (1990).
[6]M. A. Wall and A. F. Jankowski, Thin Solid Films **181**, 313 (1989).
[7]A. Moreau, J. B. Ketterson, and J. Mattson, Appl. Phys. Lett. **56**, 1959 (1990).
[8]B. M. Davis, D. N. Siedman, A. Moreau, J. B. Ketterson, J. Mattson, and M. Grimsditch, Phys. Rev. B **43**, 9304 (1991).
[9]R. C. Cammarata, T. E. Schlesinger, C. Kim, S. B. Qadri, and A. S. Edelstein, Appl. Phys. Lett. **56**, 1862 (1990).
[10]A. Moreau, J. B. Ketterson, and B. Davis, J. Appl. Phys. **68**, 1622 (1990).
[11]A. F. Jankowski and T. Tsakalakos, J. Phys. F **15**, 1279 (1985).
[12]D. Wolf and J. F. Lutsko, Phys. Rev. Lett. **60**, 1170 (1988).
[13]S. R. Phillpot and D. Wolf, Scr. Metall. **24**, 1109 (1990).
[14]R. C. Cammarata and K. Sieradzki, Phys. Rev. Lett. **62**, 2005

(1989).
[15]J. A. Jaszcak, S. R. Phillpot, and D. Wolf, J. Appl. Phys. **68**, 4573 (1990).
[16]J. P. Rogers III, P. Wynblatt, S. M. Foiles, and M. I. Baskes, Acta Metall. Mater. **38**, 177 (1990).
[17]C. M. Gilmore and V. Provenzano, Phys. Rev. B **42**, 6899 (1990); C. M. Gilmore, *ibid.* **40**, 6402 (1989).
[18]J. B. Adams, W. G. Wolfer, and S. M. Foiles, Phys. Rev. B **40**, 9479 (1989).
[19]D. Wolf, Mater. Sci. Eng. A **126**, 1 (1990); J. Appl. Phys. **69**, 185 (1991); D. Wolf and J. F. Lutsko, *ibid.* **66**, 1961 (1989); J. Mater. Res. **4**, 1427 (1989).
[20]A. Banerjea and J. R. Smith, Phys. Rev. B **35**, 5413 (1987).
[21]B. W. Dodson, Phys. Rev. B **37**, 727 (1988).
[22]J. W. Mintmire, Mater. Sci. Eng. A **126**, 29 (1990).
[23]M. S. Daw and M. I. Baskes, Phys. Rev. Lett. **50**, 1285 (1983); Phys. Rev. B **29**, 6443 (1984).
[24]S. M. Foiles, M. I. Baskes, and M. S. Daw, Phys. Rev. B **33**, 7983 (1986).
[25]S. M. Foiles, Phys. Rev. B **32**, 3409 (1985).
[26]R. S. Jones, Phys. Rev. B **41**, 3256 (1990).
[27]J. F. Lutsko, J. Appl. Phys. **65**, 2991 (1989).
[28]D. Baral, J. E. Hilliard, J. B. Ketterson, and K. Miyano, J. Appl. Phys. **53**, 3552 (1982).
[29]F. H. Streitz, K. Sieradzki, and R. C. Cammarata, Phys. Rev. B **41**, 12 285 (1990).
[30]M. Grimsditch, Phys. Rev. B **31**, 6818 (1985).